NOISE-INSENSITIVE APPROACHES TO TWO-DIMENSIONAL SYSTEM IDENTIFICATION AND TEXTURE IMAGE SYNTHESIS

Chong-Yung Chi and **Chii-Horng Chen**
Department of Electrical Engineering
National Tsing Hua Univresity
Hsinchu, Taiwan, ROC

Abstract - In this paper, Shalvi and Weinstein's 1-dimensional (1-D) computationally efficient super-exponential (SE) algorithm for blind deconvolution is extended to 2-dimensional (2-D) SE algorithm. Then a noise-insensitive 2-D blind system identification (BSI) algorithm using the computationally efficient 2-D SE algorithm is proposed for the estimation of 2-D linear shift-invariant (LSI) systems. Moreover, a texture synthesis method (TSM) using the proposed BSI algorithm is proposed for texture image synthesis. Finally, some simulation and experimental results are provided to support the efficacy of the proposed BSI algorithm and that of the proposed TSM, respectively.

1. INTRODUCTION

Assume that we are given a set of 2-D measurements $y[n_1,n_2]$

$$\begin{aligned} y[n_1,n_2] &= u[n_1,n_2] * h[n_1,n_2] + w[n_1,n_2] \\ &= \sum_{k_1=-\infty}^{\infty} \sum_{k_2=-\infty}^{\infty} h[k_1,k_2]u[n_1-k_1,n_2-k_2] + w[n_1,n_2] \quad (1) \end{aligned}$$

where $h[n_1,n_2]$ is an unknown 2-D linear shift-invariant (LSI) system, the driving input $u[n_1,n_2]$ is an unknown wide-sense stationary random field, and $w[n_1,n_2]$ is additive noise. Identification of the 2-D LSI system $h[n_1,n_2]$ with 2-D measurements $y[n_1,n_2]$ is of particular importance in a variety of 2-D signal processing applications such as 2-D spectral estimation, image modeling, coding and restoration, and texture synthesis and classification.

It is widely known that second-order statistics (correlations or power spectra [1]) can be used to extract the amplitude information of the system $h[n_1,n_2]$ such as linear prediction based methods [1], but they are blind to the system phase. Therefore, higher-order statistics, known as cumulants or polyspectra [2], that contain both the amplitude and phase information of $h[n_1,n_2]$ when measurements $y[n_1,n_2]$ are non-Gaussian, have been used for the estimation of the system $h[n_1,n_2]$.

0-7803-5650-0/99/$10.00 © 1999 IEEE

Tugnait [3] estimates $h[n_1,n_2]$ using 2-D inverse filter criteria of correlations and cumulants with application to texture synthesis. The estimate $\widehat{h}[n_1,n_2]$ is obtained as the inverse system of the optimum inverse filter $v[n_1,n_2]$. With the assumptions (a1) signal-to-noise ratio (SNR) equals infinity and (a2) the inverse system $h_{\mathrm{INV}}[n_1,n_2]$ of $h[n_1,n_2]$ is stable, he has shown that the optimum inverse filter $v[n_1,n_2] = \alpha h_{\mathrm{INV}}[n_1-\tau_1, n_2-\tau_2]$ (perfect equalization) where α is a scale factor and $[\tau_1,\tau_2]$ is a 2-D space shift. In practical applications, however, the SNR is always finite. Thus, the optimum $v[n_1,n_2]$ is affected by the noise $w[n_1,n_2]$, so is the estimate $\widehat{h}[n_1,n_2]$. Feng and Chi [4] recently reported a performance analysis of 1-D inverse filter criteria for finite SNR. They show that for finite SNR, the phase response of 1-D estimate $\widehat{h}[n]$ is equivalent to that of 1-D $h[n]$, while the lower the SNR, the more the magnitude response of $\widehat{h}[n]$ deviates from that of $h[n]$. Moreover, the optimum 1-D inverse filter $v[n]$ is obtained through a complicated and computationally expensive iterative nonlinear optimization procedure.

On the other hand, Shalvi and Weinstein [5] proposed an iterative 1-D super-exponential (SE) algorithm also using correlations and cumulants for blind channel equalization. The 1-D SE algorithm is computationally efficient since at each iteration, it finds the 1-D inverse filter $v[n]$ by solving a set of linear equations. Under the same aforementioned assumptions (a1) and (a2), the resultant 1-D $v[n]$ was shown to reduce the amount of intersymbol interference (ISI) to zero (i.e., perfect equalization) with a super-exponential rate. In this paper, we propose a 2-D SE algorithm, an extension of 1-D SE algorithm, to obtain the 2-D inverse filter $v[n_1,n_2]$. Then a computationally efficient 2-D FFT based system identification algorithm is proposed that estimates $h[n_1,n_2]$ from the obtained $v[n_1,n_2]$. The proposed 2-D system identification algorithm works well for finite (low) SNR, and the obtained estimate $\widehat{h}[n_1,n_2]$ is applied to texture image synthesis.

2. 2-D SUPER-EXPONENTIAL ALGORITHM

Assume that the given measurements $y[n_1,n_2]$ can be modeled by (1) under the following assumptions:

(A1) $u[n_1,n_2]$ is zero-mean, i.i.d., non-Gaussian with variance σ_u^2.

(A2) Both $h[n_1,n_2]$ and its inverse system $h_{\mathrm{INV}}[n_1,n_2]$ are stable LSI systems.

(A3) $w[n_1,n_2]$ is white Gaussian with variance σ_w^2 and statistically independent of $u[n_1,n_2]$.

Let the inverse filter $v[n_1,n_2]$ be an FIR filter with the region of support

$$\Omega_1[p_1,p_2] = \{[n_1,n_2] : n_1 = 0 \sim p_1, n_2 = 0 \sim p_2\} \tag{2}$$

(i.e., truncated quarter plane), and the output of $v[n_1,n_2]$ is given by

$$\begin{aligned} e[n_1,n_2] &= y[n_1,n_2] * v[n_1,n_2] \\ &= u[n_1,n_2] * g[n_1,n_2] + w[n_1,n_2] * v[n_1,n_2] \end{aligned} \tag{3}$$

where

$$g[n_1,n_2] = h[n_1,n_2] * v[n_1,n_2] \tag{4}$$

is the overall system after deconvolution.

Let

$$g'[n_1,n_2] = (g[n_1,n_2])^p (g^*[n_1,n_2])^q \tag{5}$$

$$g''[n_1,n_2] = \frac{1}{\| g'[n_1,n_2] \|} g'[n_1,n_2] \tag{6}$$

where p and q are nonnegative integers and $p+q \geq 2$, $\| x \|$ denotes 2-norm of x. Specifically, we consider the case for $p=2$ and $q=1$. As 1-D iterative SE algorithm [5], the 2-D SE algorithm iteratively forces $g[n_1,n_2]$ to converge to a delta function by updating the inverse filter $v[n_1,n_2]$ through solving the following linear equations

$$\begin{aligned} & \sum_{k=0}^{p_1}\sum_{l=0}^{p_2} v[k,l]E\{y[m,n]y^*[m+n_1-k,n+n_2-l]\} \\ = \;& \mathrm{cum}\{e[m,n],e[m,n],e^*[m,n],y^*[m-n_1,n-n_2]\} \end{aligned} \tag{7}$$

for $n_1 = 0,\cdots,p_1, n_2 = 0,\cdots,p_2$ where $\mathrm{cum}\{x_1,x_2,x_3,x_4\}$ denotes the joint cumulant of random variables x_1, x_2, x_3, x_4, and the superscript '*' denotes complex conjugation.

Next, let us present the 2-D SE algorithm in matrix form. For notational convenience, let $(n)_p$ denote "n modulo p" and $\lfloor c \rfloor$ denote the largest integer less than or equal to c. At the ith iteration, the 2-D SE algorithm obtains the unknown parameter vector

$$\mathbf{v} = (v[0,0],v[1,0]\ldots,v[p_1,0],v[0,1],v[1,1],\ldots,v[p_1,1],\ldots,v[p_1,p_2])^{\mathrm{T}} \tag{8}$$

via the following linear equations (same as (7))

$$\mathbf{v}_i = \frac{\mathbf{R}_y^{-1}\cdot\mathbf{d}_{ey}}{\|\mathbf{R}_y^{-1}\cdot\mathbf{d}_{ey}\|} \tag{9}$$

where $\mathbf{R}_y$ is a $(p_1+1)(p_2+1)\times(p_1+1)(p_2+1)$ correlation matrix with the (k,l)th element given by

$$[\mathbf{R}_y]_{k,l} = E\{y[n_1,n_2]y^*[n_1+(k-1)_{p_1+1}-(l-1)_{p_1+1}, n_2+\lfloor\frac{k-1}{p_1+1}\rfloor-\lfloor\frac{l-1}{p_1+1}\rfloor]\} \tag{10}$$

and $\mathbf{d}_{ey}$ is a $(p_1+1)(p_2+1)\times 1$ vector containing the fourth-order cross cumulant of $e_{i-1}[n_1,n_2]$ and $y[n_1,n_2]$ with the kth element given by

$$\begin{aligned}[\mathbf{d}_{ey}]_k \;=\;& \mathrm{cum}\{e_{i-1}[n_1,n_2],e_{i-1}[n_1,n_2],e^*_{i-1}[n_1,n_2], \\ & y^*[n_1-(k-1)_{p_1+1},n_2-\lfloor\frac{k-1}{p_1+1}\rfloor]\}\end{aligned} \tag{11}$$

in which $e_{i-1}[n_1,n_2]$ is the equalized signal obtained at the $(i-1)$th iteration. As the SE algorithm converges, i.e., $\| \mathbf{v}_i - \mathbf{v}_{i-1} \|^2 < \epsilon_{SE}$ where ϵ_{SE} is a small positive number, it can be shown that the obtained $\widehat{v}[n_1, n_2]$ is equivalent to $h_{\mathrm{INV}}[n_1, n_2]$ (up to a scale factor and a space shift) when SNR $= \infty$. On the other hand, when the SNR is finite and $v[n_1, n_2]$ is doubly infinite, the obtained $\widehat{v}[n_1, n_2]$ can be shown to possess the following properties:

(P1) The inverse filter $v[n_1, n_2]$ is related to the 2-D minimum mean square error (MMSE) equalizer [7], denoted $v_{\mathrm{MSE}}[n_1, n_2]$, via (in frequency-domain)

$$V(\omega_1, \omega_2) = \alpha \cdot D(\omega_1, \omega_2) V_{\mathrm{MSE}}(\omega_1, \omega_2) \tag{12}$$

where α is a positive constant, and

$$V_{\mathrm{MSE}}(\omega_1, \omega_2) = \frac{\sigma_u^2 \cdot H^*(\omega_1, \omega_2)}{\sigma_u^2 \cdot |H(\omega_1, \omega_2)|^2 + \sigma_w^2} \tag{13}$$

and $D(\omega_1, \omega_2)$ is the Fourier transform of the 2-D sequence

$$d[n_1, n_2] = g^2[n_1, n_2] g^*[n_1, n_2] \tag{14}$$

where $g[n_1, n_2]$ is given by (4).

(P2) The phase response $\arg[V(\omega_1, \omega_2)] = -\arg[H(\omega_1, \omega_2)] - \omega_1 \tau_1 - \omega_2 \tau_2$ where τ_1 and τ_2 are unknown integers.

The proof of (P1) can be easily obtained by taking Fourier transform of (7) with respect to $[n_1, n_2]$. The proof of (P2) is presented in Appendix A.

3. 2-D SYSTEM IDENTIFICATION

Let $S_{yy}(\omega_1, \omega_2)$ be the power spectrum of $y[n_1, n_2]$, and $a[n_1, n_2]$ be the associated 2-D linear prediction error (LPE) filter with the leading coefficient $a[0, 0] = 1$ and the region of support $\Omega_1[p_1, p_2]$ given by (2) or

$$\begin{aligned} \Omega_2[p_1, p_2] &= \{[n_1, n_2] : n_1 = 1 \sim p_1, n_2 = -p_2 \sim p_2\} \\ &\quad \cup \{[n_1, n_2] : n_1 = 0, n_2 = 0 \sim p_2\} \end{aligned} \tag{15}$$

(i.e., truncated asymmetric half plane). It is known [1] that for p_1 and p_2 sufficiently large, $a[n_1, n_2]$ is a whitening filter with

$$|A(\omega_1, \omega_2)|^2 \propto \frac{1}{S_{yy}(\omega_1, \omega_2)} = \frac{1}{\sigma_u^2 \cdot |H(\omega_1, \omega_2)|^2 + \sigma_w^2} \quad \text{(see (1))} \tag{16}$$

From (12), (13) and (16), it can be easily seen that

$$|H(\omega_1, \omega_2)| = \beta \cdot \frac{\Gamma(\omega_1, \omega_2)}{|D(\omega_1, \omega_2)|} \tag{17}$$

where

$$\Gamma(\omega_1, \omega_2) = |V(\omega_1, \omega_2)| / |A(\omega_1, \omega_2)|^2 \tag{18}$$

and β is a positive constant. Based on (17), an FFT based algorithm for estimating $H(\omega_1, \omega_2)$ is presented as follows:

Blind System Identification (BSI) Algorithm

Step 1 With finite data $y[n_1, n_2]$, obtain the inverse filter $v[n_1, n_2]$ using the 2-D SE algorithm presented in Section 2 and the 2-D LPE filter $a[n_1, n_2]$ using 2-D Yule-Walker equations [1]. Compute $V(\omega_1, \omega_{k_2})$, $A(\omega_{k_1}, \omega_{k_2})$ and $\Gamma(\omega_{k_1}, \omega_{k_2})$ given by (18) using $L \times L$-point 2-D FFT, where $\omega_{k_1} = 2\pi k_1/L$ and $\omega_{k_2} = 2\pi k_1/L$.

Step 2 Set $i = 0$. Set initial values $|H^{[0]}(\omega_{k_1}, \omega_{k_2})|$ for $|H(\omega_{k_1}, \omega_{k_2})|$.

Step 3 Set $i = i + 1$. Compute

$$G^{[i-1]}(\omega_{k_1}, \omega_{k_2}) = |H^{[i-1]}(\omega_{k_1}, \omega_{k_2})| \cdot |V(\omega_{k_1}, \omega_{k_2})|$$

(see (4)), and its $L \times L$-point 2-D IFFT $g^{[i-1]}[n_1, n_2]$.

Step 4 Compute $d[n_1, n_2]$ using (14) with $g[n_1, n_2] = g^{[i-1]}[n_1, n_2]$ and its $L \times L$-point 2-D FFT $D(\omega_{k_1}, \omega_{k_2})$.

Step 5 Compute $|H^{[i]}(\omega_{k_1}, \omega_{k_2})|$ using (17) then normalize it such that $\sum_{k_1} \sum_{k_2} |H^{[i]}(\omega_{k_1}, \omega_{k_2})|^2 = 1$.

Step 6 If $\sum_{k_1} \sum_{k_2} [|H^{[i]}(\omega_{k_1}, \omega_{k_2})| - |H^{[i-1]}(\omega_{k_1}, \omega_{k_2})|]^2 > \epsilon_H$, then go to Step 3; otherwise,

$$\widehat{H}(\omega_{k_1}, \omega_{k_2}) = |H^{[i]}(\omega_{k_1}, \omega_{k_2})| \cdot \exp\{-j \arg[V(\omega_{k_1}, \omega_{k_2})]\} \quad (19)$$

(up to a scale factor and a space shift) is obtained (by (P2)).

Two worthy remarks regarding the proposed BSI algorithm are as follows.

(R1) Because both the $|H(\omega_1, \omega_2)|$ estimated using (17) (see Step 5) and the phase estimate $\arg[H(\omega_{k_1}, \omega_{k_2})] = -\arg[V(\omega_{k_1}, \omega_{k_2})]$ (by (P2)) are regardless of the value of the noise variance σ_w^2. So the obtained estimate $\widehat{H}(\omega_{k_1}, \omega_{k_2})$ given by (19) is noise-insensitive.

(R2) The size of the unknown region of support for $h(n_1, n_2)$ can be arbitrary as long as the 2-D FFT size $L \times L$ is chosen sufficiently large such that aliasing effects on the resultant $\widehat{h}(n_1, n_2)$ are negligible.

4. SYNTHESIS OF TEXTURE IMAGES

Assume that we are given a texture image $x[n_1, n_2]$ (finite gray levels) that can be modeled as (1) [3]. Let $y[n_1, n_2] = x[n_1, n_2] - E\{x[n_1, n_2]\}$ (mean removed data). The proposed texture synthesis method (TSM) includes the following steps:

Step 1 Obtain the texture image model $\widehat{h}(n_1, n_2)$ and the 2-D LPE filter $A(\omega_1, \omega_2)$ using the proposed BSI algorithm.

Step 2 Estimate the MMSE equalizer (except for a scale factor) as

$$\widehat{V}_{\text{MSE}}(\omega_1, \omega_2) = \widehat{H}^*(\omega_1, \omega_2) \cdot |A(\omega_1, \omega_2)|^2 \qquad \text{(by (13) and (16))} \quad (20)$$

and obtain the MMSE estimate of the driving input by

$$u_{\mathrm{MSE}}[n_1, n_2] = y[n_1, n_2] * \widehat{v}_{\mathrm{MSE}}[n_1, n_2] \qquad (21)$$

Step 3 Generate a random field $\widetilde{u}[n_1, n_2]$ that has the same histogram as $u_{\mathrm{MSE}}[n_1, n_2]$. Then obtain a zero-mean synthetic texture image by

$$\widetilde{y}[n_1, n_2] = \widetilde{u}[n_1, n_2] * \rho\widehat{h}[n_1, n_2] \qquad (22)$$

where the scale factor ρ is determined such that $E\{|\widetilde{y}[n_1, n_2]|^2\} = E\{|y[n_1, n_2]|^2\}$.

Step 4 The synthetic texture image $\widetilde{x}[n_1, n_2] = \widetilde{y}[n_1, n_2] + E\{x[n_1, n_2]\}$ is quantized into finite gray levels as those of $x[n_1, n_2]$.

5. SIMULATION AND EXPERIMENTAL RESULTS

In this section, we present some simulation results in Example 1 and some experimental results in Example 2 to support the efficacy of the proposed BSI algorithm and that of TSM, respectively. The proposed BSI algorithm was employed in these two examples with $|H^{[0]}(\omega_{k_1}, \omega_{k_2})| = 1$, FFT size $L \times L = 256 \times 256$ and convergence parameters $\epsilon_{SE} = 10^{-3}$ and $\epsilon_H = 10^{-5}$.

Example 1. Simulation results

In the example, $u[n_1, n_2]$ was assumed to be a zero-mean, exponentially, i.i.d. random field with variance $\sigma_u^2 = 1$ and $h[n_1, n_2]$ was a 2-D quarter plane causal AR(4,4) model taken from [6]. The synthetic $y[n_1, n_2]$ was generated for data size equal to 256 × 256 and SNR = 5 dB. The same region of support $\Omega_1[4,4]$ for both the 2-D inverse filter $v[n_1, n_2]$ and the 2-D LPE filter was used. The true $h[n_1, n_2]$ and the average of thirty independent estimates $\widehat{h}[n_1, n_2]$ are shown in Figures 1(a) and 1(b), respectively. One can see, from these figures, that the proposed BSI algorithm can provide an accurate estimate for the system $h[n_1, n_2]$.

Example 2. Experimental results

In the example, the region of support for the 2-D inverse filter $v[n_1, n_2]$ was $\Omega_1[4,4]$, while that for the 2-D LPE filter was $\Omega_2[4,4]$. Four texture images, grass, wood, raffia and sand with size 128 × 128 taken from USC-SIPI (University of Southern California - Signal and Image Processing Institute) Image Data Base were used for texture synthesis. The experimental results including original texture images and the synthetic texture images are shown in Figures 2(a) through 2(h). From these figures, one can see that the synthetic texture images quite resemble the original texture images.

6. CONCLUSIONS

We have presented a noise-insensitive and computationally efficient BSI algorithm for the estimation of 2-D LSI systems and a TSM using the proposed BSI. Some simulation results that support the former and some experimental results that support the latter were presented. The proposed BSI works well even for low SNR as long as the data length is sufficiently large.

ACKNOWLEDGMENTS

This work is supported by the National Science Council under Grant NSC-88-2218-E-007-019.

Appendix A - Proof of (P2)

Proving (P2) is equivalent to proving that the overall system $G(\omega_1,\omega_2)$ is zero phase assuming $\tau_1 = \tau_2 = 0$ without loss of generality. The proof to be presented below needs the following two assumptions

(B1) $g[n_1,n_2] \neq 0$ only for $[n_1,n_2] \in \Omega[N,N]$ and $g[0,0] > 0$ where

$$\Omega[p_1,p_2] = \{[n_1,n_2] : n_1 = -p_1 \sim p_1, n_2 = -p_2 \sim p_2\} \qquad (23)$$

(B2) $0 < |g[N,N]| < |g[n_1,n_2]|$, $\forall [n_1,n_2] \in \Omega[N,N]$, $[n_1,n_2] \neq [N,N]$ and $[n_1,n_2] \neq [-N,-N]$.

Let

$$\begin{aligned} f[n_1,n_2] &= d[n_1,n_2] * g^*[-n_1,-n_2] \\ &= \sum_{m_1=-N}^{N} \sum_{m_2=-N}^{N} g[m_1,m_2]|g[m_1,m_2]|^2 g^*[m_1-n_1,m_2-n_2] \\ &\qquad\qquad \text{(by (B1))} \qquad (24) \end{aligned}$$

It can be easily shown, from (12) and (13) that the 2-D Fourier transform $F(\omega_1,\omega_2) = D(\omega_1,\omega_2)G^*(\omega_1,\omega_2) \geq 0$ which implies $f[n_1,n_2] = f^*[-n_1,-n_2]$ and $f[0,0] \geq |f[n_1,n_2]|$.

Note, from (24), that $f[n_1,n_2] \neq 0$ only for $[n_1,n_2] \in \Omega[2N,2N]$, and that

$$\begin{aligned} f[2N,2N] &= |g[N,N]|^2 g[N,N] g^*[-N,-N] \\ &= f^*[-2N,-2N] = |g[-N,-N]|^2 g[-N,-N] g^*[N,N] \quad (25) \end{aligned}$$

which leads to

$$|g[N,N]| = |g[-N,-N]| \qquad (26)$$

Next, let us consider $f[2N,2N-1] = f^*[-2N,-2N+1]$ that leads to

$$\begin{aligned} & g[N,N]g^*[-N,-N+1]\{|g[-N,-N+1]|^2 - |g[N,N]|^2\} \\ = \;& g^*[-N,-N]g[N,N-1]\{|g[N,N-1]|^2 - |g[-N,-N]|^2\} \quad (27) \end{aligned}$$

which by (B2) and (26), further gives rise to

$$|g[N,N-1]| = |g[-N,-N+1]| \tag{28}$$

and

$$\frac{g[N,N]}{g^*[-N,-N]} = \frac{g[N,N-1]}{g^*[-N,-N+1]} \tag{29}$$

Similarly, letting $f[n_1,n_2] = f^*[-n_1,-n_2]$ given by (24) for $n_1 = N+1,\cdots,2N$, $n_2 = 0,\cdots,2N$ and $n_1 = N, n_2 = N,\cdots,2N$, one can end up with

$$|g[n_1,n_2]| = |g[-n_1,-n_2]|, \ \forall[n_1,n_2] \in \Omega[N,N] \tag{30}$$

and

$$\frac{g[n_1,n_2]}{g^*[-n_1,-n_2]} = \frac{g[0,0]}{g^*[0,0]} = 1, \ \forall[n_1,n_2] \in \Omega[N,N] \tag{31}$$

(since $g[0,0] > 0$ by (B1)) that implies

$$g[n_1,n_2] = g^*[-n_1,-n_2], \ \forall[n_1,n_2] \in \Omega[N,N] \tag{32}$$

In other words, $g[n_1,n_2]$ is zero phase, and we thus have completed the proof for (P2) under the two assumptions (B1) and (B2). However, the two assumptions can be relaxed by letting $N \to \infty$ for (P2) to be true.

References

[1] S.M. Kay, *Modern Spectral Estimation,* Englewood Cliffs, Prentice Hall, 1988.

[2] C.L. Nikias and A.P. Petropulu, *Higher-Order Spectra Analysis: a Nonlinear Signal Processing Framework*, Englewood Cliffs, Prentice-Hall, 1993.

[3] J.K. Tugnait, "Estimation of linear parametric models of non-Gaussian discrete random fields with application to texture synthesis," *IEEE Trans. Image Processing*, vol. 3, no. 2, pp. 109-128, Mar. 1994.

[4] C.-C. Feng and C.-Y. Chi, "Performance of cumulant based inverse filters for blind deconvolution," to appear in *IEEE Trans. Signal Processing*, July 1999.

[5] O. Shalvi and E. Weinstein, "Super-exponential methods for blind deconvolution," *IEEE Trans. Inform. Theory*, vol. 39, no. 2, pp. 504-519, Mar. 1993.

[6] S. R. Parker and A. H. Kayran, "Lattice parameter autoregressive modeling of two-dimensional fields- Part I: The quarter-plane case," *IEEE Trans. ASSP*, vol. 32, no. 4, pp. 872-885, Aug. 1984.

[7] M.H. Hayes, *Statistical Digital Signal Processing and Modeling*, John Wiley and Sons, New York, 1996.

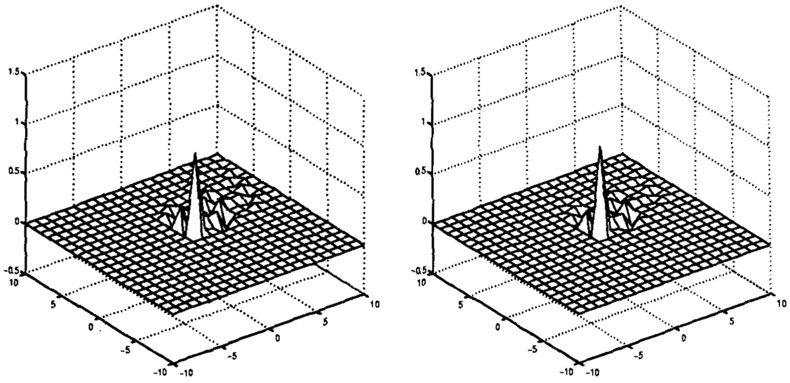

Fig. 1(a) **Fig. 1(b)**

Figure 1. Simulation results of example 1. (a) The true system $h[n_1, n_2]$; (b) the average of thirty independent estimates $\widehat{h}[n_1, n_2]$.

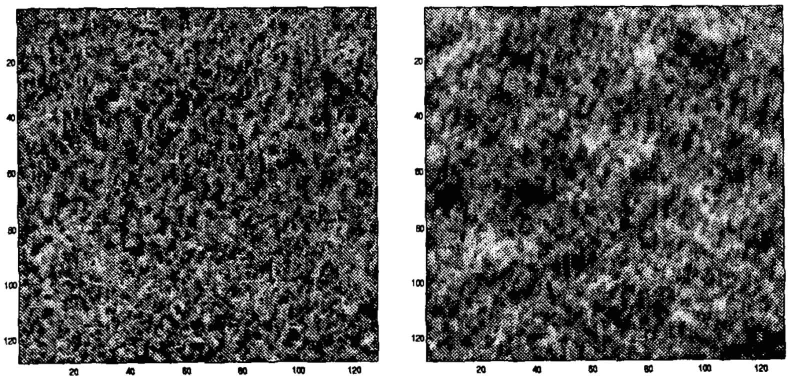

Fig. 2(a) **Fig. 2(b)**

Figure 2. Experimental results of Example 2. Original and synthetic texture images: (a) grass and (b) synthetic grass image.

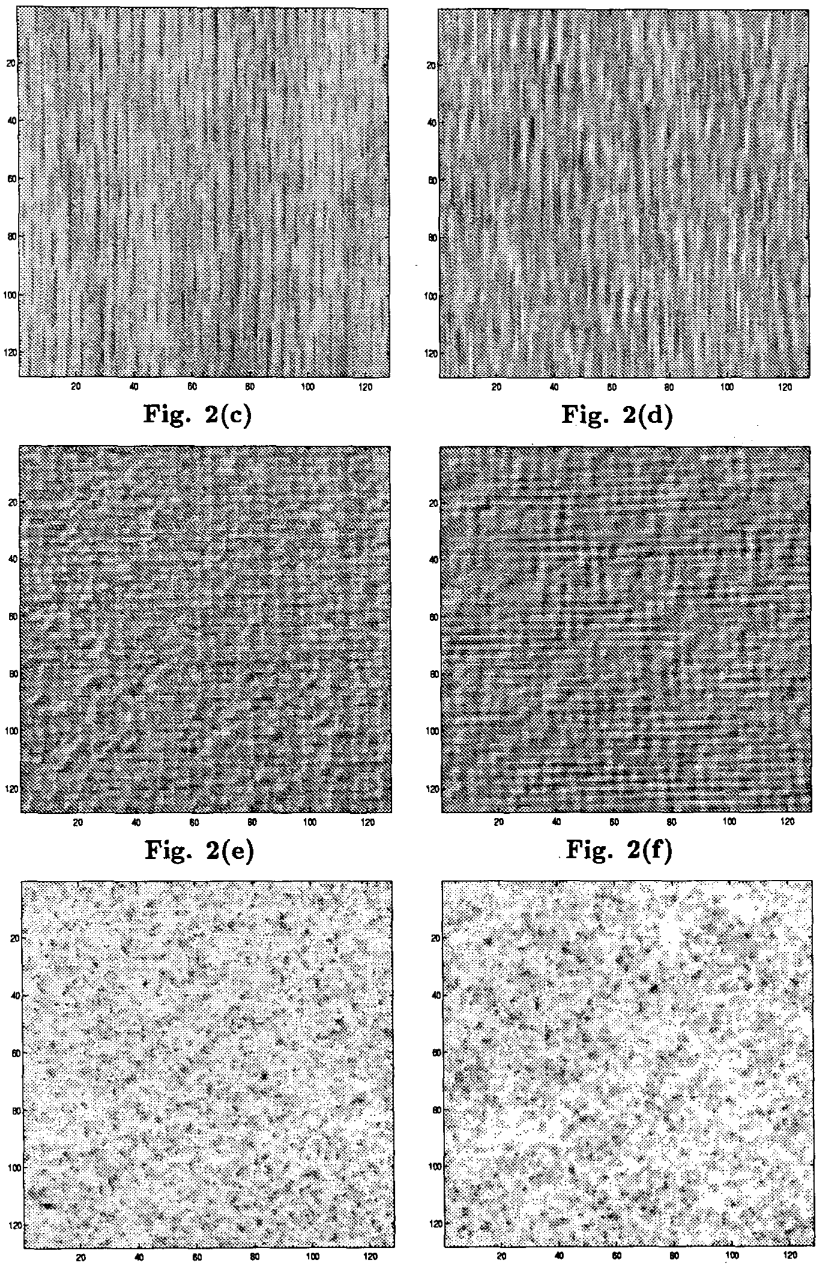

Fig. 2(c)

Fig. 2(d)

Fig. 2(e)

Fig. 2(f)

Fig. 2(g)

Fig. 2(h)

Figure 2. (Continued) Experimental results of Example 2. Original and synthetic texture images: (c) wood and (d) synthetic wood image; (e) raffia and (f) synthetic raffia image; (g) sand and (h) synthetic sand image.